Fizika Nizkikh Temperatur, 2003, v. 29, No. 8, p. 835–839

Simulation of stochastic vortex tangle*

L.P. Kondaurova, S.K. Nemirovskii, and M.V. Nedoboiko

Kutateladze Institute of Thermophysics SB RAS, Novosibirsk 630090, Russia
E-mail: theory@itp.nsc.ru

Received December 19, 2002

We present the results of simulation of the chaotic dynamics of quantized vortices in the bulk of superfluid He II. Evolution of vortex lines is calculated on the base of the Biot–Savart law. The dissipative effects appeared from the interaction with the normal component, or/and from relaxation of the order parameter are taken into account. Chaotic dynamics appears in the system via a random forcing, e.i. we use the Langevin approach to the problem. In the present paper we require the correlator of the random force to satisfy the fluctuation-dissipation relation, which implies that thermodynamic equilibrium should be reached. In the paper we describe the numerical methods for integration of stochastic differential equation (including a new algorithm for reconnection processes), and we present the results of calculation of some characteristics of a vortex tangle such as the total length, distribution of loops in the space of their length, and the energy spectrum.

PACS: 47.32.Cc, 67.40.Vs, **05.40.–a**

1. Introduction

Quantized vortices appearing in quantum fluids influence many properties of the systems. In general, the set of these vortices represents a chaotic vortex tangle (VT) consisting of separated vortex loops (closed vortex lines). To describe the influence of VT, it is necessary to know the statistical description of VT at various moments of time evolution because at different processes quantized vortices reveal the different properties: thermodynamical equilibrium and nonequilibrium (turbulent). For example quasi-equilibrium features are essential in the process of fast quenching. In turn, in experiments with thermal flows and/or counterflows in He II a set of the vortices shows very nonequilibrium (turbulent type) properties. The statistical descriptions of these two cases are strongly different. Thus the distribution of vortex loops on their length $n(l) = dN(l)/dl$ is governed by the formula [1] $n(l) \propto l^{-5/2}$ in the case of the thermal equilibrium, while in turbulent helium we have [2] $n(l) \propto l^{-4/3}$. There exist many works devoted to numerical investigations of vortex tangles and to turbulent state of helium, e.g. [3–10]. Let's note that the mentioned calculations have been done in the local approximation framework. Originally simple vortex structures (VS) with time turn into a very strongly tangled system. If a self-crossing of the filaments happens in this system, the reconnection of vortex line occurs and thus the vortex loops divide or confluence. Reconnections change the topology of vortex structures and affect the evolution of a VT. In the papers mentioned above, reconnection was simulated from the condition of the equality between the local and nonlocal contributions to the velocity of a vortex filament point, i.e., $v_{nl} \approx \approx \kappa/2\pi\Delta \approx v_l \approx c\kappa \ln(R/a_0)/4\pi R$, where $\Delta = 2R/[c \times \times \ln(R/a_0)]$ is the minimal distance between the pair of vortices, κ is the quantum of circulation, R is the radius of curvature at the given point, c is the constant ($\simeq 1$), and a_0 is the cutting parameter concerning with the radius of the vortex core. Thus, in those works only the distance between the points of a vortex line was chosen as the criterion for reconnection. In our opinion, this is slightly incorrect approach, because the elements of filaments can go away from each other and the crossing may not occur. In contrast to the mentioned above papers, we consider the entire Biot–Savart equation. Moreover, we take into ac-

* The report was submitted at the 3rd International Workshop on Low Temperature Microgravity Physics (CWS-2002).

© L.P. Kondaurova, S.K. Nemirovskii, and M.V. Nedoboiko, 2003

count possible random disturbances in the system of vortices. The disturbances are simulated by addition of a new term to the Biot—Savart equation. The details see below. This statement is conventional for the description of dynamical systems with stochastical perturbations. Moreover, in this work the following condition of reconnections is proposed: if the elements of a VT have intersected during the temporal step of the calculation, the reconnection occurs.

2. The problem statement and the dynamical equation

We consider the dynamics of vortex loops in three-dimensional infinite space. The induced velocity of helium at a point r is defined by the Biot—Savart law:

$$\mathbf{v}(\mathbf{r}) = \frac{\kappa}{4\pi}\int \frac{(\mathbf{S}-\mathbf{r})\times d\mathbf{s}}{|\mathbf{S}-\mathbf{r}|^3} .$$

The formulae for the velocity of vortex line points, while without dissipation, takes the form [3]:

$$\frac{d\mathbf{s}}{dt} = \dot{\mathbf{S}}_0 = \frac{\kappa}{4\pi}\int \frac{(\mathbf{S}_1-\mathbf{S})\times d\mathbf{S}_1}{|\mathbf{S}_1-\mathbf{S}|^3} + $$

$$+\frac{\kappa}{4\pi}\ln\left(\frac{2\sqrt{S_+S_-}}{e^{1/4}\cdot a_0}\right)\mathbf{S}'\times\mathbf{S}'', \qquad (1)$$

where $\mathbf{S}(\xi\,,t)$ is the radius-vector of the vortex line points, ξ is a parameter, in this case the arclength, $\mathbf{S}'$ is the arclength derivative, S_+ and S_- are the lengths of two adjacent line elements that hold the point $\mathbf{s}$ between, and the prime denotes differentiation with respect to the arclength ξ . The second term of Eq. (1) is the local part of the velocity the first term is the nonlocal part obtained by integration on the rest of the vortex line and on all of the other loops. Taking into account the frictional force of vortices and the normal component of helium and the rapidly fluctuating random term (Langevin's force), we obtain the equation for the dynamics of a point of the vortex line:

$$\dot{\mathbf{S}} = \dot{\mathbf{S}}_0 + \alpha\,[\mathbf{S}'\times(\mathbf{v_n}-\dot{\mathbf{S}}_0)] -$$

$$-\alpha'\mathbf{S}'\times[\mathbf{S}'\times(\mathbf{v_n}-\dot{\mathbf{S}}_0)] + A(t,\xi), \qquad (2)$$

where

$$\langle A(t,\xi)\rangle = 0,\ \langle A_i(t_1,\xi_1)A_j(t_2,\xi_2)\rangle =$$

$$= D\delta_{ij}\delta(t_1-t_2)\delta(\xi_1-\xi_2) = D\delta_{ij}\delta(\xi_1-\xi_2)\langle n(t)n(t')\rangle ,$$

i, j are the spatial components; t_1, t_2 are the arbitrary time moments; ξ_1, ξ_2 define any points on the vortex line; D is the intensity of the Langevin's force; α, α' are the friction coefficients; $n(t)$ is the Gaussian white noise with $\langle n(t)\rangle = 0$, $\langle n(t)n(t')\rangle = \delta\,(t-t')$. Let's assume further that the difference between the normal and the superfluid velocities of helium equals to zero $\mathbf{v}_n = 0$ and neglect the term with α'. This statement correspond to absence of a heat flow. Thus, finally we obtain the dynamical equation for a vortex line:

$$\dot{\mathbf{S}} = \dot{\mathbf{S}}_0 - \alpha\mathbf{S}'\times\dot{\mathbf{S}}_0 + \sigma(\xi)n(t) . \qquad (3)$$

In the integral form Eq. (3) is as follows:

$$\mathbf{S}(t,\xi) = \mathbf{S}(t_0,\xi) + \int_{t_0}^{t}\mathbf{B}(\xi\,,t)dt + \sigma(\xi)\int_{t_0}^{t}dW, \qquad (4)$$

where $\mathbf{B}(\xi\,,t) = \dot{\mathbf{S}}_0 - \alpha\mathbf{S}'\times\dot{\mathbf{S}}_0$, and $W(t) = \int_{t_0}^{t} n(t')dt$ is the standard Wiener process. In our model the initial conditions is six completely symmetrical rings with orientation making the total impulse of the system equal to zero.

3. The numerical algorithm and the description of reconnections

The Eq. (4) was solved by the Euler method:

$$S_{n+1} = S_n + hB(\xi\,,t_n) + \sqrt{h}\sigma(\xi)\eta_n ,$$

where S_n is the approximate solution of the equation in a mesh point on time t_n; h is the integration step on time in a mesh point t_n; $\{\eta_n\}$ is the consistency of independent between itselves normal random vectors with independent between itselves components in the aggregate $\eta_{n,j}$ $(j = 1, 2, 3)$, having zero expectation value and the dispersion is 1. The component of vector η_n was calculated by formula: $\eta_{n,j} = \sqrt{-2\ln\alpha_1}\,\times$ $\times\cos(2\pi\alpha_2)$, where α_1 and α_2 is random numbers from the interval (0,1) obtained by a pseudorandom-number generator. The Euler method is the first order on the mean-square approximation in the time step. The functions $\mathbf{S}', \mathbf{S}'', \dot{\mathbf{S}}_0$ were calculated as in paper [3]. To keep the calculation procedure coherent, points on the vortex line were added and removed was carry out as in the work [10].

The first step in the modeling of a reconnection process is selection of point pairs that are the candidates for reconnection. After the pairs was defined, it was assumed that the line segments between each of the pairs were moving with a constant velocity (according V_i, V_j) during the time step, as illustrated in Fig. 1.

From the compatibility of equations

$$x_i + V_{x,i}h + (x_{i+1} - x_i)s1 =$$

$$= x_j + V_{x,j}h + (x_{j+1} - x_j)s;$$

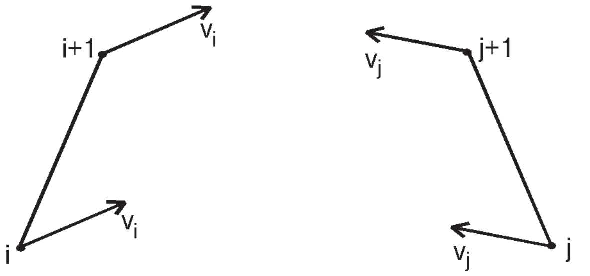

Fig. 1. The elements of vortex lines must to reconnect.

$$y_i + V_{y,i}h + (y_{i+1} - y_i)s1 =$$
$$= y_j + V_{y,j}h + (y_{j+1} - y_j)s;$$
$$z_i + V_{z,i}h + (z_{i+1} - z_i)s1 =$$
$$= z_j + V_{z,j}h + (z_{j+1} - z_j)s;$$
$$0 \le s1 \le 1; \quad 0 \le s \le 1$$

it was determine the meeting of these line segments during the time step. Here $(x_i, y_i, z_i,\ x_{i+1}, y_{i+1}, z_{i+1})$; $(x_j, y_j, z_j,\ x_{j+1}, y_{j+1}, z_{j+1})$ are the coordinates of the first and the second pairs of points, accordingly; $V_{x,i}, V_{y,i}, V_{z,i}; V_{x,j}, V_{y,j}, V_{z,j}$ are the projections of the velocities of the points and the line segments on the coordinate axis. If the line segments had met, the reconnection occurs. Thus, if originally the points belong to the same loop, a pair of new loops was generated. Otherwise the confluence of the loops occurs.

4. The results

The initial radii of rings were $R = 2 \cdot 10^{-5}$ m. The initial condition was chosen in a way that the total impulse of the system was equal to zero. The rings were situated symmetrically at equal distance in pairs around the coordinate origin. The distance between them was $d = 10^{-5}$ m. The parameters in Eq. (2) are $\alpha = 0.0098$, $D = 4 \cdot 10^{-5}$ m/s.

Simulation was performed with a constant temporal step $h = 5 \cdot 10^{-8}$ s and initial steps along the vortex line was $\Delta l_0 = 2\pi \cdot 10^{-7}$ m. The steps Δl along the vortex line was controlled later by the procedure of inserting and removing of points, so that $\Delta l_0/2 \le \Delta l \le 2\Delta l_0$. It follows from Eq. (4) that small (or those with a high curvature) loops move very rapidly and their dissipation (decrease in the size) is very high due to the friction. Therefore, small loops were removed during our calculations. Kinks appearing on vortex lines were removed also. For our case, the loops were cancelled if there were less than 5 points.

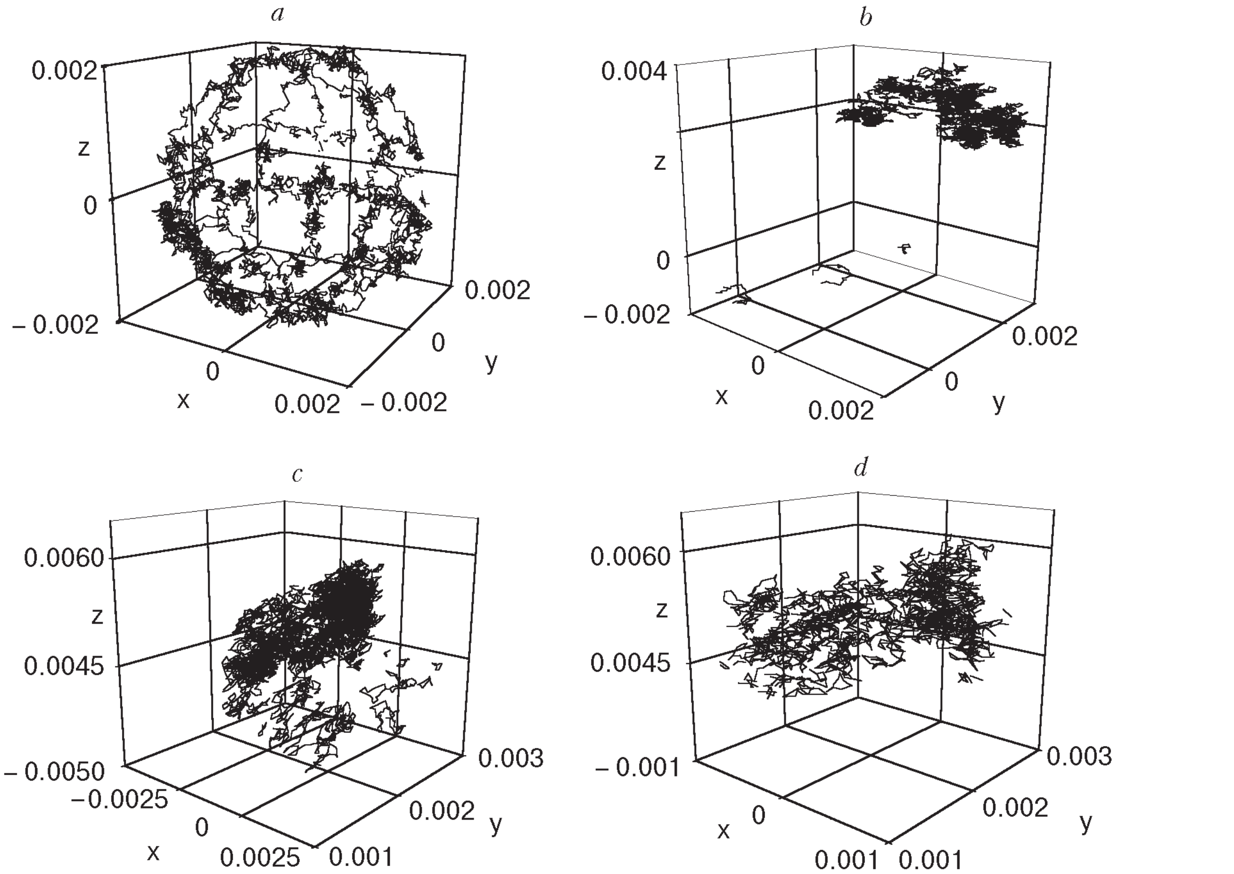

Fig. 2. The vortices at different times t, s: $4.30 \cdot 10^{-5}$ (*a*), $9.792 \cdot 10^{-4}$ (*b*), $1.0892 \cdot 10^{-3}$ (*c*), $1.1444 \cdot 10^{-3}$ (*d*). The configurations are plotted in a three-dimensional view.

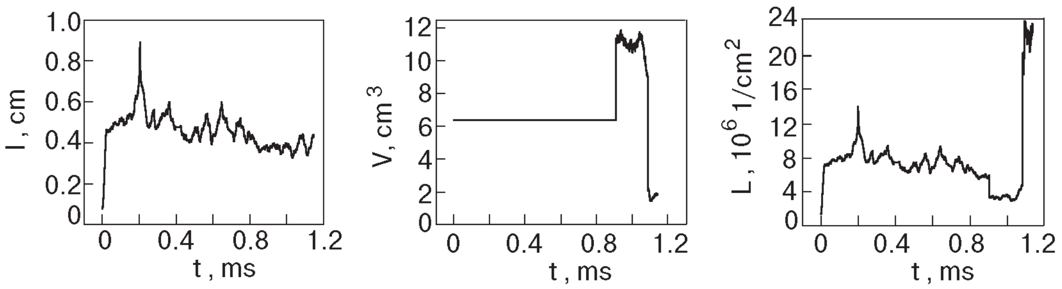

Fig. 3. Plots of the total lines l, the volume V, filed with vortices, and the vortex lines density L as functions of time.

Vortex configurations at various time moments are presented in Fig. 2. One can see a vortex structure with drastic evolution in time. After numerous time steps the system evolved into separated vortex tangles. It was noted that during the evolution, the vortex tangles arose and then vanished in different places. It resembles us the favor intermittency phenomenon in classical turbulence.

From the simulation, several quantities were calculated and plotted as functions of time (see Fig. 3). One can see the phases of evolution for vortex structures. At the beginning, the total length, averaged curvature, and the vortex lines density increase at a steady volume. After a certain value of the density has been archived, many of small loops developers and the VT begin to decay. Later, one can observe a tendency to a fluctuating steady state. However, after the time $t = 9.792 \cdot 10^{-4}$ s, the volume suddenly begin to decrease. It is conform to disappearance of detached loops (see Fig. 2,*c*,*d*). Then again the fluctuating steady state is reached.

We made also calculations for some statistical characteristics of a VS. The distribution of the loop number vs. its length and the VC energy spectrum were calculated. Figure 4 shows the distribution of vortex loops on their length at the time region $t \approx 1.1443$ s. Decreasing of the loops amount is described by the following function: $n(l)dl \sim l^{-0.93}$. The same dependence was observed both for different times and for each vortex tangle within the vortex structure. It is difficult to extract physically meaningful results from this data. On the one hand, the equilibrium has been reached. On the other hand, the distribution of vortex loops disagrees with the results obtained for thermal equilibrium and turbulent stationary state.

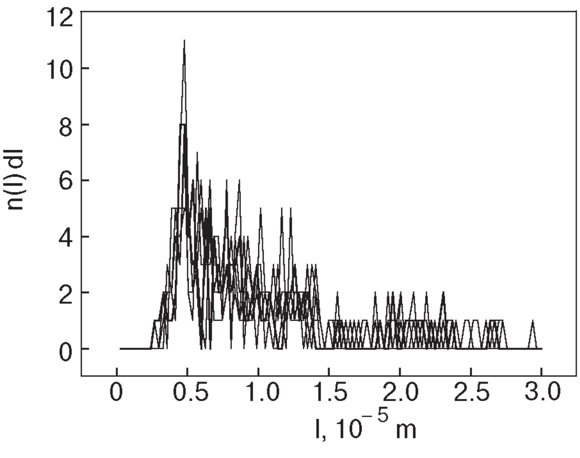

Fig. 4. The distribution of the vortex loops on their length at the time region $t \approx 1.1443$ s.

The average kinetic energy of flow induced by a vortex loop can be evaluated as follows [11]:

$$E = \left\langle \int \frac{\rho_s V_s^2}{2} d^3 r \right\rangle =$$

$$= \int\limits_k \frac{d^3k}{4\pi k^2} \left\langle 2\pi\rho_s \kappa^2 \int\limits_0^{L'} \int\limits_0^{L} \mathbf{S}(\xi_1)\dot{\mathbf{S}}(\xi_2) \times \right.$$

$$\left. \times \exp\{-ik\,[\mathbf{S}(\xi_1) - \mathbf{S}(\xi_2)]\}\, d\xi_1 d\xi_2 \right\rangle = \int\limits_0^{\infty} E(k)dk,$$

$$E(k) = \frac{\rho_s \kappa^2}{2(2\pi)^3} \int \frac{d\Omega_k}{k^2} \int\limits_0^{L} \int\limits_0^{L'} \dot{\mathbf{S}}(\xi_1)\dot{\mathbf{S}}(\xi_2) \times$$

$$\times \exp\{-i\mathbf{k}\,[\mathbf{S}(\xi_1) - \mathbf{S}(\xi_2)]\}\, d\xi_1 d\xi_2,$$

where $d\Omega_k = k^2 \sin\theta_k d\theta_k d\Phi_k$ is the elementary volume, $\mathbf{k}$ is the wave vector, and ρ_s is the superfluid density. For the isotropic case, the spectral density is expressed as follows:

$$E(k) = \frac{\rho_s \kappa^2}{(2\pi)^2} \int\limits_0^{L} \int\limits_0^{L'} \frac{\sin(k\,|\mathbf{S}(\xi_1) - \mathbf{S}(\xi_2)|)}{k\,|\mathbf{S}(\xi_1) - \mathbf{S}(\xi_2)|} [d\mathbf{S}(\xi_1) \cdot d\mathbf{S}(\xi_2)],$$

where k is the wave number. It is seen that there exist different regions of wave number k: small with respect to $(V)^{1/3}$, high with respect to $1/\sqrt{L}$, and intermediate values. In the region of small wave numbers, $E(k) \propto k^2$, and for high numbers, $E(k) \propto k^{-1}$.

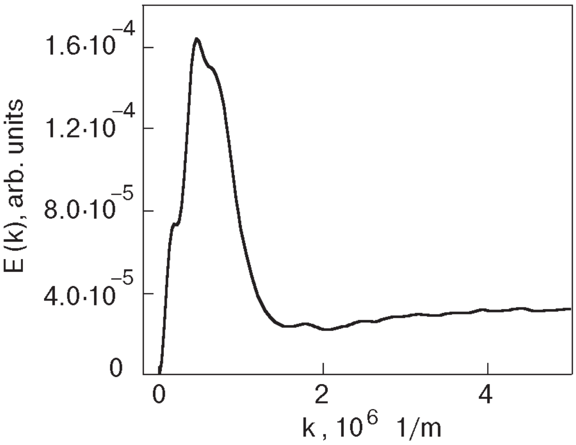

Fig. 5. The energy spectrum of the vortex tangle at $t = 1.1445 \cdot 10^{-3}$ s.

Figure 5 shows our numerical results of the VC spectral density for the time $t = 1.1445 \cdot 10^{-3}$ s . In the region of small wave numbers, simulation data fits the approximation $E(k) \propto k^2$. In the region of high wave numbers, it is difficult to extract a regularity from this data, since the spectral density and the numerical error are of the same scale. In the intermediate region, the energy decreases according to the formula: $E(k) \propto k^{-2.9}$.

5. Conclusion

The obtained numerical results demonstrate that initially smooth vortex rings transform into a highly chaotic vortex tangle. In spite of that total length fluctuates about a constant value, we think that the thermal equilibrium state has not been reached yet. For instance, the spectral density of the energy agrees with the equipartition law only for a small k-zone. The vortex loop distribution on their length also differs from the one expected for a thermal equilibrium. This state is closer to the turbulent case observed by other authors. During evolution the vortex tangles arise and disappear in different places. It resembles the favor intermittency phenomenon in classical turbulence. Our preliminary simulation demonstrates that the Langevin approach applied in this paper is a very promising method for study of chaotic vortex structures.

The work is supported by INTAS grant 2001-0618.

1. N.D. Antunes and L.M.A. Bettencourt, *Phys. Rev. Lett*. **82**, 2824 (1999).
2. T. Araki, M. Tsubota, and S.K. Nemirovskii (to be published).
3. K.W. Schwarz, *Phys. Rev.* **B31**, 5782 (1985).
4. P.G. Saffman, *Stud. Appl. Math*. **49**, 371 (1970).
5. M.E. Agishtein and A.A. Migdal, *Modern Phys. Lett*. **A1**, 221 (1986).
6. K.W. Schwarz, *Phys. Rev*. **B38**, 2398 (1988).
7. T.F. Buttke, *J. Comp. Phys.* **76**, 301 (1988).
8. D.C. Samuelse, *Phys. Rev*. **B46**, 11714 (1992).
9. M. Tsubota and S. Mackawa, *J. Low Temp. Phys*. **89**, 4411 (1992).
10. R.G.M. Aarts, *A Numerical Study of Quantized Vortices in He II*, Tech. Univer. Eindhoven (1993).
11. S.K. Nemirovskii, *Phys. Rev*. **B57**, 5792 (1997).